ANALYTICAL SCIENCES JUNE 2020, VOL. 36

Introduction of Air-Segmentation Approach to Flow Titration by Feedback-based and Subsequent Fixed Triangular Wave-controlled Flow Ratiometry

Junya Ochiai,* Sawako Oka,* Tomoko Hirasaka,* Erina Tomiyama,* Hiroya Kubo,* Kazumasa Okamoto,* Masaki Takeuchi,*, and Hideji Tanaka*,**†**

**Faculty of Pharmaceutical Sciences, Tokushima University, 1-78-1 Shomachi, Tokushima 770–8505, Japan*
***Institute of Biomedical Sciences, Tokushima University, 1-78-1 Shomachi, Tokushima 770–8505, Japan*

An air-segmentation approach has been introduced to a feedback-based and subsequent fixed triangular wave-controlled flow ratiometry to suppress axial dispersion in flow titration. The flow rate of a base solution containing an indicator is linearly varied with a control signal, V_c, supplied by a computer. The solution is merged with an acid solution under a constant total flow rate. Air is introduced to the merged solution in order to segment the solution with air bubbles. Both phases are led to a UV/Vis detector without phase separation. Air signals are removed by signal processing. The effect of the lag time between the merging of solutions upstream and the sensing of the corresponding signal downstream is offset by feedback-based upward and downward V_c scans, and thus the V_c that gives the equivalence composition is determined. Subsequently, fixed triangular wave control is applied to a narrower V_c range with a higher scan rate to enhance the throughput rate (maximally 11.8 titrations/min). Air-segmentation has been found to be effective to reduce axial dispersion and to preserve the titrand/titrant composition upon their just being merged. Consequently, the applicable range is extended especially to lower titrand concentration. The proposed method has been successfully applied to various acid-base titrations, including the nonaqueous titration of the Japanese Pharmacopoeia drug.

Keywords Flow titration, flow ratiometry, feedback-based control, triangular wave control, air-segmentation, nonaqueous titration

(Received October 22, 2019; Accepted December 10, 2019; Advance Publication Released Online by J-STAGE December 20, 2019)

Introduction

Titrimetry is a classical analytical method that is still in use widely because of its advantages, such as high precision and versatility. Titrimetry is an absolute method, which can be traced to SI units (*i.e.*, kg and mol) without relying on a calibration curve. In the field of pharmaceutical sciences, the 17th Japanese Pharmacopoeia[1] adopts titrimetry as quantitation methods for nearly half of the drugs listed. However, conventional manual titration needs a long time (typically 5 – 10 min/titration) and considerable amounts of the titrand and titrant. Manual titration is not realistic when the number of samples to be analyzed is large. Therefore, various flow titrimetries, including flow injection (FI) titration,[2] sequential injection (SI) titration,[3] triangle programmed coulometric titration[4] and so on, have been developed, as reviewed by Tanaka and Nakano.[5] More recently, Wójtowicz *et al*.[6] reported an FI titration coupled with a merging zone method. Del Rio[7] applied chemometrics to the second-order signals, obtained by an SI titration with a diode allay-UV/Vis detector, to extract analyte signals in the presence of other absorbent species. Lima *et al*.[8,9] reported a digital movie-based detection using a webcam for automatic titration with a flow-batch analyzer. Lima and Reis[10] applied multicommuted flow analysis to photometric titration for the measurement of food sample acidity. Paengnakorn *et al.*,[11] studied toward green titration based on an SI-Lab-at-Valve approach for downscaling. Néri-Quiroz *et al*.[12] reported a miniaturized titration in a microfluidic capillary column system. Karita and Kaneta applied microfluidic paper-based analytical devices to acid-base[13] and chelatometric[14] titrations.

Blaedel and Laessig developed a "continuous automated buretless titrator" and applied it to redox[15] and chelatometric[16] titrations. In their method, the titrand and titrant were merged at various flow ratios, while the former flow rate was kept constant. The flow ratio was converged within 5 min to give an analytical signal that corresponded to the equivalence signal. The lag time (t_{lag}) from the merging the solutions upstream and the sensing corresponding analytical signal downstream was the major reason for limiting the throughput rate. Their approach can be regarded as being a prototype of the flow ratiometry of the present study.

Dasgupta *et al*.[17–20] proposed an on-line true titration based on a feedback-based flow ratiometry. The effect of t_{lag} was corrected by repeating upward and downward scans of the flow ratio. The scan was limited to just the range of interest through a feedback-based control. Their approach realized high throughput titration of 18.7 titrations/min (*i.e.*, 3.2 s/titration).[17] Recently, Fais *et al*.[21] employed this concept to construct a

† To whom correspondence should be addressed.
E-mail: h.tanaka@tokushima-u.ac.jp

sensor-controlled flow apparatus for online titration. Aydan *et al.*[22] simultaneously determined magnesium and calcium ions by a feedback-based flow ratiometry using a photosensor and an ion sensor that were set in series in a flow system. Tanaka *et al.*[23-25] further enhanced the throughput rate of flow ratiometry by combining a feedback-based control with a subsequent fixed triangular wave control that scanned a narrower range with a higher rate. Miyazaki *et al.*[26] realized an unprecedented throughput rate of 46.9 titrations/min (1.28 s/titration) by applying this concept.

It is important for flow ratiometry to acquire analytical signals that accurately reflect the titrand/titrant composition upon their just being merged. Sasaki *et al.*[27] reported a tracer-monitored titration, where a dye tracer was used to estimate an accurate titrand/titrant flow ratio or concentration gradient after dispersion. To reduce the axial dispersion in the conduit is also effective to acquire reliable results. In previous studies,[28-30] we introduced an air-segmentation approach[31,32] to amplitude modulated multiplexed flow analysis,[33] our original concept of flow analysis. The axial dispersion was limited within each liquid segment being separated by air bubbles. Both liquid and air phases were led to a detector without any physical phase separation.[30] Instead, air signals were removed by a signal processing. Air-segmentation with software-based deaeration was effective for limiting the axial dispersion and for improving the sensitivity.

In the present study, the concept of air-segmentation with software-based deaeration[30] was introduced to a flow ratiometry. After the analytical parameters were optimized, the method was applied to titrations of various acids and bases including nonaqueous titration of the 17th Japanese Pharmacopoeia drug. The applicable range was found to extend to a lower titrand concentration by air-segmentation.

Experimental

Reagents and chemicals

The reagents used in the present study were purchased from Kanto Chemicals (Tokyo, Japan), Nacalai Tesque (Kyoto, Japan) or Wako Pure Chemical Industries (Osaka, Japan). The reagents were used without further purification. Bulk powder of isoniazid (ISCOTIN®) and fine granules of 4% furosemide (Lasix®) were the 17th Japanese Pharmacopoeia drugs, and were purchased from Daiichi Sankyo Co. and Nichi-Iko Pharmaceutical Co., respectively. The drugs were, respectively, dissolved in acetic acid–acetic anhydrate (5:1 in volume ratio) and *N*,*N*-dimethylformamide. Zartorius Ariumm 611 DI-grade deionized water was used throughout.

Flow system

Figure 1 shows the flow system configured in the present study. The system involves a three-channel manifold. Polytetrafluoroethylene (PTFE) tubing with an inner diameter (i.d.) of 0.5 mm was used as a conduit in the upstream side of a segmenter (Seg; BL Tec Inlet Block 178-B482-02, Japan). On the other hand, PTFE tubing with a slightly larger i.d. (0.8 mm) was used in the downstream side in order to coalesce fine air bubbles to form air bubbles with software processible dimension. Three peristaltic pumps (P_1 and P_2: Rainin Dynamax RP-1, USA; P_3: Gilson Miniplus 3 MP-2, USA), each having 10 stainless-steel rollers, were used to deliver solutions or air. The flow rate (F_B) of a base solution containing an acid-base indicator was varied over the range from 0 to 1.43 cm^3 min^{-1} with P_1 in response to the controller output voltage (V_c, 0 – 5 V)

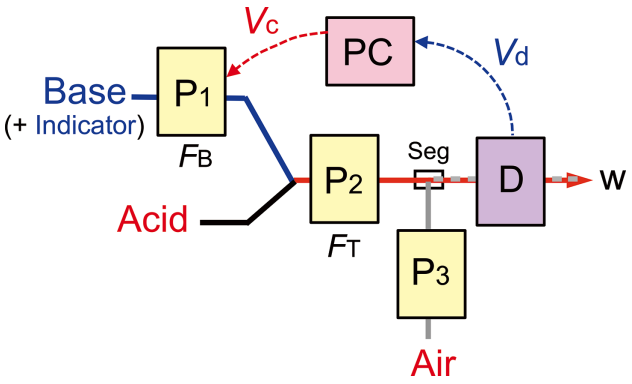

Fig. 1 Flow system for flow titration by flow ratiometry coupled with an air segmentation approach. P_1 – P_3, peristaltic pumps; Seg, segmenter; D, UV/Vis detector; PC, laptop computer with A/D-D/A converter; w, waste; F_B, flow rate of base solution; F_T, total flow rate of merged solution; V_c, control signal; V_d, detector output signal.

supplied from a laptop computer (PC; Toshiba Dynabook Satellite 1850 SA120C/4, Japan) through an A/D-D/A converter (Measurement Computing PC-CARD DAS16/12-AO, USA). Some experiments in the later part of the study were carried out by using a new set of a computer (HP ProBook 430 G3, USA) and a converter (CONTEC USB I/O Terminal AIO-160802GY-USB, Japan) because of a breakdown of the above-mentioned converter (discontinued model). An acid solution was aspirated from the second channel at a flow rate of $F_T - F_B$, where F_T is the total liquid flow rate (1.43 cm^3 min^{-1}) controlled with P_2, and merged with the base solution. The merged solution was segmented by air bubbles, which were introduced from the third channel at a flow rate of 0.48 cm^3 min^{-1}. In addition to the active mixing by the rollers of P_2, circulation within each liquid segment[34-37] is considered to facilitate the mixing of titrand and titrant. In a preliminary experiment, no appreciable difference was observed between the analytical values obtained with and without a knitted tubing reactor[37] of 20, 30, 40 and 50 cm in length. No mixing reactor was, therefore, used in the present flow system. Both the liquid and air phases were led to a handmade flow cell (quartz tubing with an optical path length of 1 mm) that was mounted in the optical cell compartment of a spectrophotometer (Shimadzu SPD-6AV UV/Vis, Japan) (D). The absorbance at the maximum absorption wavelength of the base form of the indicator was measured. The output voltage (V_d) from the detector, sampled at a frequency of 20 Hz, was quantized by the converter and acquired in PC as the Microsoft Excel format. As for the new set of computer and converter, 10 Hz was selected as the frequency because it could reduce the file size, while keeping good analytical performance.

Principle

The principle of feedback-based and subsequent fixed triangular wave-controlled flow ratiometry was described in detail before.[23-25] Therefore, the following is a brief description on the principle; a detailed description is provided in Supporting Information (Fig. S1 and its caption). The titrand/titrant flow ratio is continuously changed by linearly changing V_c. Initially, feedback-based control (FB) is applied. In this mode, the V_c scan direction is reversed at the instant when V_d corresponding to the equivalence point (V_{sp}) is sensed. Upward and downward scans of V_c can offset the effect of t_{lag} and locate the equivalence

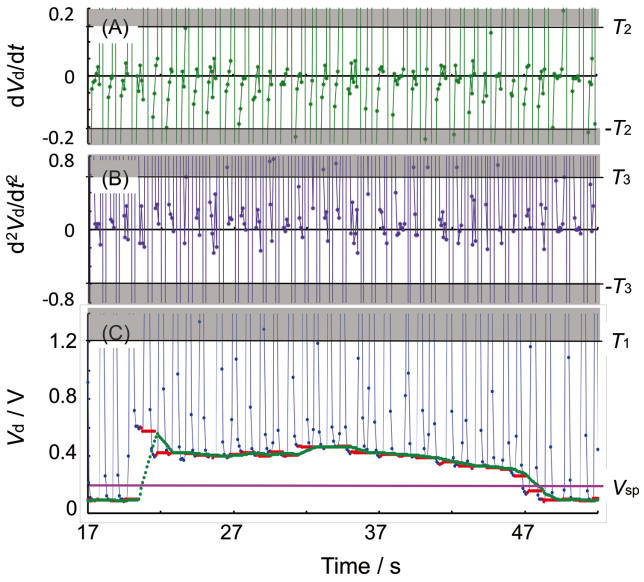

Fig. 2 Scheme of software-based deaeration. Titrand, 0.05 mol dm^{-3} HCl; titrant, 0.1 mol dm^{-3} NaOH containing 0.047 mmol dm^{-3} Bromothymol Blue. (A) Threshold value, T_2, for the first derivative of raw V_d signals. (B) Threshold value, T_3, for the second derivative of raw V_d signals. (C) Threshold value, T_1, for the deviation of acquired V_d from the latest liquid V_d. V_{sp}, V_d corresponding to the equivalence point. Sampling frequency was 10 Hz. When any of ΔV_d, $|dV_d/dt|$ or $|d^2V_d/dt^2|$ with regard to an acquired V_d (plots in blue) exceeded corresponding threshold values (T_1, T_2 and T_3, respectively) as displayed by shadowed area, the V_d was regarded as air signal and discarded. Thus, deaerated signals were obtained (plots in red). Moving average computation was further applied to the obtained signals for smoothing. As a result, deaerated and smoothed V_d was obtained as shown in green in Fig. 2C.

control signal (V_E). Next, fixed triangular wave control (Fxd) is put into operation. In this mode, the V_c scan is carried out in narrower range with a higher rate than in the preceding FB mode to further increase the throughput rate.

Figure 2 shows the principle of the software-based deaeration by using real data, where 0.05 mol dm^{-3} HCl was titrated with 0.1 mol dm^{-3} NaOH containing 0.047 mmol dm^{-3} Bromothymol Blue (BTB). In a previous study,[30] air and liquid phases were rather easily identified because air bubbles gave a steep peak-shaped V_d. Two kinds of threshold values, the deviation (ΔV_d) of acquired V_d from the latest liquid V_d (T_1) and the slope (dV_d/dt) of the acquired V_d from the latest raw V_d (T_2), were sufficient for the phase recognition. In the present study, however, the liquid phase as well as air bubbles gave a steep V_d slope around the equivalence point due to the color transition of the indicator. Even in such a transition range, air bubbles gave a still steeper V_d than the liquid phase. The third threshold vale (T_3 in Fig. 2B) was, therefore, set for the second derivative (d^2V_d/dt^2) of V_d signals in order to emphasize the difference of the slopes between the air V_d and the liquid V_d, and thus to facilitate phase recognition. To determine the three kinds of threshold values, the data were carefully analyzed by enlarging the air–liquid interfacial region in the graphs, as shown in Fig. 2. Firstly, the T_1 value was determined because it was easy to visually recognize peak-shaped air signals. Next, T_2 and then T_3 were determined after some trials and errors in order to make the phase recognition more complete. When any of the ΔV_d, $|dV_d/dt|$ or $|d^2V_d/dt^2|$ with regard to an acquired V_d (plots in blue in Fig. 2C) exceeded the corresponding threshold values (T_1, T_2 and T_3, respectively, in Fig. 2), V_d was regarded as being air signal, and discarded. In this case, the latest liquid V_d was held instead of the acquired V_d. This process resulted in a stairway V_d profile (plots in red in Fig. 2C). A moving average computation was, therefore, applied to the deaerated V_d for smoothing. As a result, software deaerated and smoothed V_d signals were obtained, as shown in green in Fig. 2C. In the period shown in this figure (35 s), 33 air segments were recognized; 255 data points among a total of 351 data were regarded as air signals. The signals for air–liquid interface are considered to be sorted as air signals.

Software

The analytical procedures (*i.e.*, controlling the system, acquiring/analyzing the data and displaying the results) were fully automated by using software written in house, except for a manual change of the samples. Initially, a program written in Excel VBA Ver. 7.0 was used. It works by an interpreter system, which translates the code when it executes the orders. Later, a new program written in Visual BASIC 2017, which was suitable to the new A/D-D/A converter and computer (see the section of *Flow system*), was developed with Visual Studio IDE. It works by a compile system, which translates the code to machine language before execution of the program. The developed software consists of four classes named MainForm for manipulating Graphical User Interface, ExcelFileServer for recording data in Microsoft Excel sheet, DataCollector for acquiring V_c and V_d as digital data and ContecADDAConverter for interfacing between the computer and the converter. Figure S2 (Supporting Information) shows an example of the MainForm, where 0.1 mol dm^{-3} HCl is titrated with 0.1 mol dm^{-3} NaOH.

Results and Discussion

Optimization of control signal

The scan rate of V_c in the FB and Fxd modes and the scan range of V_c in the latter mode were investigated without air-segmentation. The results are listed in Table S1 (Supporting Information), where 0.05 mol dm^{-3} HCl (A) and 0.08 mol dm^{-3} CH_3COOH (B) were titrated with 0.1 mol dm^{-3} NaOH. In the FB mode, the time needed per titration is $2t_{lag}$.[17] The t_{lag} consists primarily of the transit time of the solution from the confluence point to the optical window of the flow cell and minutely of the sensor's response time. Therefore, the time required per titration was almost independent of the scan rate. Even so, a higher scan rate is more preferable for quickly locating the new equivalence point when the titrand concentration is considerably changed and the FB mode is started again. Therefore, 100 mV s^{-1} was selected as the V_c scan rate in the FB mode because the precision of V_E became slightly lower at a higher scan rate (Table S1(B)).

On the other hand, the time needed per titration is proportional to the V_c scan range and inversely proportional to the V_c scan rate in the Fxd mode.[23–25] Table S2 (Supporting Information) shows the results on the effect of the V_c scan range, where the scan rate of V_c was held at 100 mV s^{-1}. The range was expressed as the percentage of the V_c scan range in the Fxd mode to that in the preceding FB mode. Therefore, if 50% is selected, the V_c scan is carried out in the range from $V_E - 0.25\ (V_H - V_L)$ to $V_E + 0.25\ (V_H - V_L)$, where V_E, V_H and V_L are the latest values in the preceding FB mode. Narrower range (*i.e.*, 10%) could not give stable results. The time needed per titration was almost

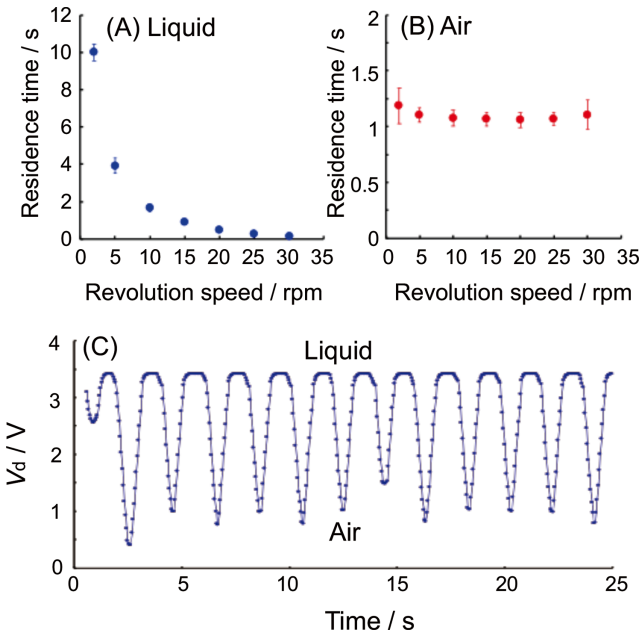

Fig. 3 Effect of the revolution speed of P_3 on the residence time of 0.05 mmol dm^{-3} Erythrosine B segment (A) and on that of air bubble (B) in optical window. (C) Analytical signals at a P_3 revolution speed of 15 rpm. Sampling frequency was 20 Hz.

proportionally increased with the scan range, as expected. By taking the throughput rate and precision into account, 50% was selected as the V_c scan range in the Fxd mode.

Table S3 (Supporting Information) lists the results on the V_c scan rate in the Fxd mode. The higher is the scan rate, the shorter is the time per titration. The determination coefficients (r^2) for the linear regression line of time/titration *vs*. the reciprocal of V_c scan rate were 0.996 and 0.999 for the titrations of HCl and CH_3COOH, respectively, and in accordance with the theory.[23–25] Although a higher throughput rate could be achieved when the V_c scan rate was 400 mV s^{-1}, 200 mV s^{-1} was selected because it gave more precise results.

Optimization of air-segmentation

The air flow rate was investigated for a precise segmentation of the liquid stream by air bubbles. For this purpose, Base channel in Fig. 1 was closed and 0.05 mmol dm^{-3} Erythrosine B or 0.15 mmol dm^{-3} Tartrazine, respectively known as food dyes Red No. 3 and Yellow No. 5, were delivered from the Acid channel at a flow rate of 1.43 cm^3 min^{-1}. The analytical wavelengths for the dyes were 526 and 428 nm, respectively. Air was introduced with P_3 that revolved at 2, 5, 10, 15, 20, 25 or 30 rpm. The volumes of the liquid segment and the air bubble was estimated from their respective residence times in the optical window and the whole (liquid + air) flow rate. Figures 3A and 3B show the relationships between the P_3 revolution speed and the residence time of the Erythrosine B solution (A) or air bubble (B). The residence time of the liquid segment was decreased with the revolution speed for air introduction (A). On the other hand, the dependency of the air bubble size on the pump speed seems to be rather minimal (B). Similar results were obtained for Tartrazine. As a result, 15 rpm was selected as the optimum revolution speed because it allowed sufficiently small liquid segment formation and precise air bubble introduction. The flow rate of air delivered with P_3 at 15 rpm, estimated by a water displacement method, was 0.48 cm^3 min^{-1}. Figure 3C shows the analytical signals at the optimized condition (*i.e.*, 15 rpm). The average volume of liquid segments and air bubbles estimated were 28.6 ± 2.2 and 33.9 ± 1.9 mm^3, respectively.

Table 1 Typical analytical parameters

Parameter	Selected value
Flow rate, P_1	0 – 1.43 cm^3 min^{-1}
P_2	1.43 cm^3 min^{-1}
P_3	0.48 cm^3 min^{-1}
Scan rate of V_c, FB mode	100 mV s^{-1}
Fxd mode	200 mV s^{-1}
Scan range of V_c in Fxd mode	$V_E \pm 0.25\ (V_H - V_L)$[a]
Sampling frequency	20 Hz
Number of data for moving average	13
Threshold values, T_1 for V_d	1.2 V
T_2 for dV_d/dt	0.15 V s^{-1}
T_3 for d^2V_d/dt^2	0.6 V s^{-2}
Set point (V_{sp})[b]	0.1 V

a. Latest V_E, V_H and V_L value in the preceding feedback mode.
b. Detector output voltage V_d corresponding to the equivalence point.

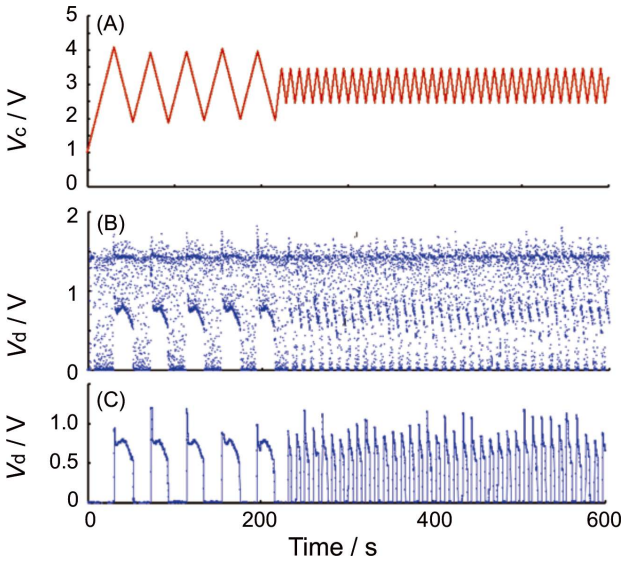

Fig. 4 Typical flow signals. (A) Control voltage, V_c. (B) Raw detector output voltage, V_d. (C) Software-based deaerated and smoothed V_d. Titrand, 0.1 mol dm^{-3} HCl; titrant, 0.1 mol dm^{-3} NaOH containing 0.047 mmol dm^{-3} Bromothymol Blue. Sampling frequency was 20 Hz.

Table 1 summarize the analytical parameters selected, where the values of T_2, T_3 and V_{sp} are the most typical values and need some adjustment, if necessary, depending on the species and concentration of the indicator used.

Analytical performance

Figures 4A and 4B, respectively, show typical V_c and raw V_d signals, where 0.1 mol dm^{-3} HCl was titrated with 0.1 mol dm^{-3} NaOH containing 0.047 mol dm^{-3} BTB. As shown in Fig. 4A, feedback-based control with a V_c scan rate of 100 mV s^{-1} was executed initially. At the instant when V_{sp} was determined 10 times (t = 216.4 s), fixed triangular wave control with a higher scan rate (200 mV s^{-1}) was applied to a narrower range (*i.e.*, $V_c = V_E \pm 0.25\ (V_H - V_L)$), where V_E, V_H and V_L were the latest

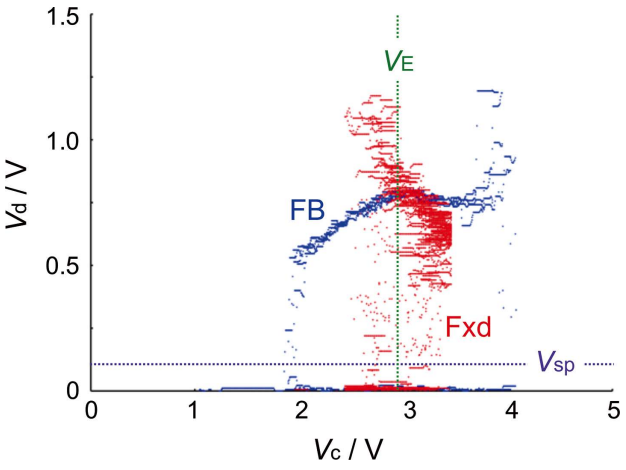

Fig. 5 Titration curve for the data given in Fig. 5. FB, data obtained in feedback-based mode; Fxd, data obtained in fixed triangular wave-controlled mode; V_E, controller output voltage that gives equivalence composition at the confluence point; V_{sp}, V_d corresponding to the equivalence point.

Table 2 Application to various acid-base titration

Titrand	Titrant[a]	Indicator[b]	λ_{anal}/ nm	Range/ mol dm^{-3}	Linearity, r^2
HCl	NaOH	BTB	618	0.01 – 0.3	0.994
CH_3COOH	NaOH	TB	596	0.01 – 0.5	0.995
H_3PO_4, 1st	NaOH	BCG	616	0.015 – 0.5	0.998
2nd	NaOH	TP	594	0.015 – 0.5	0.992
NaOH	HCl	BTB	618	0.025 – 0.3	0.998
NH_3	HCl	BCG	616	0.025 – 0.3	0.999
Na_2CO_3, 1st	HCl	TB	596	0.025 – 0.3	0.999
2nd	HCl	BCG	616	0.025 – 0.3	0.999
Isoniazid[c]	$HClO_4$[d]	PNB	630	0.01 – 0.2	0.999
Furosemide[e]	NaOH	BTB	618	0.016 – 0.05	0.980

V_{sp} (V_d regarded as the equivalence point signal) was set at 0.1 V except for Isonizid (0.024 V) and Furosemide (0.38 V).
a. Titrant concentration: 0.1 mol dm^{-3}.
b. BTB, Bromothymol Blue; TB, Thymol Blue; BCG, Bromocresol Green; TP, Thymolphthaleine; PNB, *p*-Naphtolbenzein,
c. 17th ed. Japanese Pharmacopoeia drug. Dissolved in acetic acid.
d. Dissoved in acetic acid–acetic anhydrate (5:1 in volume ratio).
e. 17th ed. Japanese Pharmacopoeia drug. Dissoved in *N*,*N*-dimethyl-formamide.

equivalence V_c (2.951 V), maximum V_c (3.960 V) and minimum V_c (1.943 V) in the just preceding FB mode, respectively. Raw V_d signals (Fig. 4B) were scattered over a wide range from –0.03 to 1.82 V because they contained both liquid and air signals. As shown in Fig. 4C, air signals could be removed through the signal processing described in Principle; 3040 data points among total 4329 data points were regarded as air signals. The throughput rates are 2.92 titrations/min (= 20.6 s/titration) and 11.82 titrations/min (= 5.1 s/titration) in the FB and Fxd modes, respectively. The sample throughput is less than these values, because repeating measurements are necessary in general for each sample, as with conventional manual titrations. The present method would exercise its advantage of the high-throughput nature when it is applied to the continuous monitoring of a stream changing concentration, such as those reported before.[17,18] The V_E values of 2.95 ± 0.04 V (n = 7) and 2.94 ± 0.06 V (n = 71) in the FB and Fxd modes, respectively, agreed well.

Figure 5 shows the relationship between V_c and V_d for the data shown in Fig. 4. This figure is regarded as a titration curve in conventional batch titration, because V_c determines the flow rate of the titrant (*i.e.*, $F_B = kV_c$, where k is a proportional constant). In contrast to conventional titration curve, the curve is of loop profile because of t_{lag}. That is, V_c further increased or decreased when its corresponding analytical signal was sensed after t_{lag}. This shows that the scan range of V_c in the Fxd mode is narrower (half of that in the FB mode). In addition, the scan rate of V_c in the Fix mode was twice as fast as that in the FB mode. These facts contributed to the higher throughput rate in the Fxd mode, as mentioned above. The repeatability of data, especially those obtained in the Fxd mode, are seemingly not very good. However, the RSD values of V_E were only 1.35 and 2.05% in the FB and Fxd modes, respectively.

In principle, flow ratiometry is an absolute method that needs no calibration curve, as long as the flow rates are accurately calibrated.[17] However, the construction of a calibration curve is more practical than a laborious calibration of the flow rates. V_E is expressed by the following equation:[17]

$$\frac{1}{V_E} = \frac{kn_BC_B}{F_Tn_AC_A} + \frac{k}{F_T}. \quad (1)$$

Here, n, C and F are the valency, concentration and flow rate, respectively, of solutions denoted by the subscripts (A, acid; B, base; T, acid + base). Therefore, the plot of V_E^{-1} against C_A^{-1} (if acid is titrand) or C_B (if base is titrand) gives a linear calibration curve. The calibration curves for the titration of HCl with 0.1 mol dm^{-3} NaOH obtained by the present air-segmented flow ratiometry and the previous non-segmented flow ratiometry are shown in Fig. S4 (Supporting Information). This shows that the linearity of the calibration curve has been greatly improved (r^2 = 0.999) by introducing an air segmentation technique. The effect of air segmentation is more significant in a low concentration range of the titrand. The calibration curve obtained by the previous method curvatured and deviated downwards from a linear relationship when the concentration of HCl is lower than 0.02 mol dm^{-3} (*i.e.*, $C_{HCl}^{-1} > 50$ mol^{-1} dm^3).

Application to various acid-base titraions

The developed method was applied to titrations of various acids and bases, including the Japanese Pharmacopoeia drugs (isoniazid and furosemide). The titrant was 0.1 mol dm^{-3} HCl or NaOH, except for isoniazid. Regardless of titrand or titrant, acid and base solutions were fed from the channels respectively denoted Acid and Base in Fig. 1. The scan range and the scan rate were the same as those listed in Table 1. Acid-base indicators were selected by referring both the transition interval of the indicator and the estimated pH at the equivalence point. Therefore, as for the titrations of H_3PO_4 and Na_2CO_3, the first and the second equivalence points could be determined independently by selecting an appropriate indicator for each equivalence point. The results are listed in Table 2. It shows that the present method can be applied to various acid-base titrations. The titration of isoniazid was carried out in nonaqueous media, where the titrand and titrant ($HClO_4$) were dissolved in acetic acid and acetic acid-acetic anhydrate (5:1 in volume ratio), respectively. Figure S4 (Supporting Information) shows flow signals for the titration of 0.03 mol dm^{-3} isoniazid with 0.1 mol dm^{-3} $HClO_4$ with or without air-segmentation. It shows the transition of V_d became steeper through the suppression of axial dispersion by air-segmentation. Non segmented flow ratiometry (previous method) was unable to

determine a lower concentration of isoniazid (0.02, 0.016 and 0.01 mod dm^{-3}) because V_d could not reach to V_{sp} due to the axial dispersion. On the other hand, air-segmented flow ratiometry (present method) could successfully be applied to such lower concentrations.

Acknowledgements

The present study was partly supported by a Grant-in-Aid for Scientific Research (C) (15K07889) from the Japan Society for the Promotion of Sciences (JSPS).

Supporting Information

The principle of the feedback-based and subsequent fixed triangular wave-controlled flow ratiometry is described in detail in Fig. S1. An example of the MainForm display of the newly developed Visual Basic software is shown in Fig. S2. Examples of the flow signals for the nonaqueous titration of 0.03 mol dm^{-3} isoniazid with 0.1 mol dm^{-3} $HClO_4$ with and without air segmentation are shown in Fig. S3. A comparison of the calibration curves for the titration of HCl with 0.1 mol dm^{-3} NaOH, obtained by air-segmented flow ratiometry (present method) and non-segmented flow ratiometry (previous method), is shown in Fig. S4. The results concerning the optimization for the V_c scan rate and the V_c scan range are compiled in Tables S1 – S3. These materials are available free of charge on the Web at http://www.jsac.or.jp/analsci/.

References

1. "The Japanese Pharmacopoeia Seventeenth Edition", **2016**, The Ministry of Health, Labor and Welfare, Tokyo.
2. A. U. Ramsing, J. Ruzicka, and E. H. Hansen, *Anal. Chim. Acta*, **1981**, *129*, 1.
3. J. F. van Staden and H. du Plessis, *Anal. Commun.*, **1977**, *34*, 147.
4. G, Nagy, K. Tóth, and E. Pungor, *Anal. Chem.*, **1975**, *47*, 1460.
5. H. Tanaka and T. Nakano, *J. Flow Injection Anal.*, **2004**, *21*, 123.
6. M. Wójtowicz, J. Kozak, K. Danielewska, and P. Kościelniak, *Talanta*, **2009**, *76*, 1006.
7. V. del Río, M. S. Larrechi, and M. P. Callao, *Talanta*, **2010**, *81*, 1572.
8. R. A. C. Lima, L. F. Almeida, W. S. Lyra, L. A. Siqueira, E. N. Gaião, S. S. L. Paiva Junior, and R. L. F. C. Lima, *Talanta*, **2016**, *147*, 226.
9. L. A. Siqueira, I. S. Nunes, P. L. A. Almeida Junior, W. S. Lyra, R. A. N. Andrade, M. C. U. Araújo, L. F. Almeida, and R. A. C. Lima, *Microchem. J.*, **2017**, *133*, 593.
10. M. L. A. Lima and B. F. Reis, *Microchem. J.*, **2017**, *135*, 207.
11. P. Paengnakorn, S. Chanpaka, K. Watla-Iad, W. Wongwilai, and K. Grudpan, *Anal. Sci.*, **2019**, *35*, 219.
12. J. Néri-Quiroz, F. Canto, L. Guillerme, L. Couston, A. Magnaldo, and V. Vegas, *Talanta*, **2019**, *196*, 237.
13. S. Karita and T. Kaneta, *Anal. Chem.*, **2014**, *86*, 12108.
14. S. Karita and T. Kaneta, *Anal. Chim. Acta*, **2016**, *924*, 60.
15. W. J. Blaedel and R. H. Laessig, *Anal. Chem.*, **1964**, *36*, 1617.
16. W. J. Blaedel and R. H. Laessig, *Anal. Chem.*, **1965**, *37*, 332.
17. H. Tanaka, P. K. Dasgupta, and J. Huang, *Anal. Chem.*, **2000**, *72*, 4713.
18. P. K. Dasgupta, H. Tanaka, and K. D. Jo, *Anal. Chim. Acta*, **2001**, *435*, 289.
19. P. K. Dasgupta and K. D. Jo, *Electroanalysis*, **2002**, *14*, 1383.
20. K. D. Jo and P. K. Dasgupta, *Talanta*, **2003**, *60*, 131.
21. M. Fais, C. Schwarz, and F. C. Leinwebr, *Chem. Ing. Tech.*, **2016**, *88*, 793.
22. T. Aydan, A. Kitagawa, M. Takeuchi, and H. Tanaka, *J. Flow Injection Anal.*, **2008**, *25*, 65.
23. H. Tanaka and T. Baba, *Talanta*, **2005**, *67*, 848.
24. H. Tanaka and T. Baba, *Anal. Sci.*, **2005**, *21*, 615.
25. N. Kakiuchi, A. Miyazaki, A. Fujikawa, M. Takeuchi, and H. Tanaka, *J. Flow Injection Anal.*, **2017**, *34*, 11.
26. A. Miyazaki, N. Kakiuchi, K. Okamoto, M. Takeuchi, and H. Tanaka, *J. Flow Injection Anal.*, **2019**, *36*, 97.
27. M. K. Sasaki, D. L. Rocha, F. R. P. Rocha, and E. A. G. Zagatto, *Anal. Chim. Acta*, **2016**, *902*, 123.
28. K. Inui, T. Uemura, T. Ogusu, M. Takeuchi, and H. Tanaka, *Anal. Sci.*, **2011**, *27*, 305.
29. H. Yoshida, K. Inui, M. Takeuchi, and H. Tanaka, *Anal. Sci.*, **2012**, *28*, 523.
30. T. Ogusu, K. Uchimoto, M. Takeuchi, and H. Tanaka, *Talanta*, **2014**, *118*, 123.
31. L. T. Skeggs, *Am. J. Clin. Pathol.*, **1957**, *28*, 311.
32. L. T. Skeggs, *Anal. Chem.*, **1966**, *38*, 31A.
33. H. Tanaka, T. Mima, M. Takeuchi, and H. Iida, *Talanta*, **2008**, *77*, 576.
34. L. R. Snyder and H. J. Adler, *Anal. Chem.*, **1976**, *48*, 1017.
35. L. R. Snyder and H. J. Adler, *Anal. Chem.*, **1976**, *48*, 1022.
36. E. H. Hansen, "*Advances in Flow Injection and Related Techniques*", ed. S. D. Kolev and I. D. McKelvie, **2008**, Chap. 1, Elsevier, Amsterdam, 25.
37. V. Cerdà and J. M. Estela, "*Advances in Flow Analysis*", ed. M. Trojanowicz, **2008**, Chap. 2, Wiley-VCH, Weinheim, 45.
38. J. Ruzicka and E. H. Hansen, "*Flow Injection Analysis*", 2nd ed., **1988**, John Wiley & Sons, New York, 31.